Optimal guidance for Toss Back concepts of Reusable Launch Vehicles

Elliot Brendel⋆*, Bruno Hérissé*⋆ *and Eric Bourgeois*⋆⋆
⋆*DTIS, ONERA, Université Paris Saclay*
F-91123 Palaiseau, France
elliot.brendel@onera.fr, bruno.herisse@onera.fr
⋆⋆*CNES Launcher Directorate, DLA/SDT/SPC*
52, rue Jacques Hillairet, 75012 Paris, France
eric.bourgeois@cnes.fr

Abstract

In the context of the development of future launchers, Toss Back concepts are being studied by CNES together with ONERA. Focusing on the recovery phase between end of ascent and start of the landing boost, a guidance algorithm using an indirect method of optimal control based on Pontryagin's Maximum Principle is presented. First, a reference trajectory is computed offline, then this trajectory is used to initialize the guidance algorithm which consists in recomputing the optimal control online. Promising results have shown their benefits. In particular, solutions are provided quickly, at a frequency that is compatible with embedded guidance components.

1. Introduction

In the context of the development of future launchers, various innovative concepts of Reusable Launch Vehicles are being studied by CNES,[3] together with ONERA, for the recovery of the first stage of the vehicle. Among the large number of such concepts, the Vertical Take-off and Vertical Landing (VTVL) or Toss Back strategy is based on the re-ignition of the rocket propulsion engine for the landing to the launch site. Since much energy is lost to make the vehicle return, this simple concept, which was adopted for SpaceX Falcon 9, is rather suitable for highly vertical ascent trajectories to minimize propellant consumption during the return flight. Nevertheless, finding trajectories minimizing propellant mass consumption remains fundamental for such a recovery approach. Moreover, due to uncertainties on parameters (rocket engine, aerodynamic coefficients, etc.) and uncertainties on the environment (wind, air density, atmospheric pressure), dispersions of the state of the vehicle can grow along the trajectory, mainly at end of the ascent and at the re-entry.[4] Then, it is necessary to compute such optimal strategies online and in real time. In this paper, a numerical algorithm is provided for optimal guidance from the stage separation to the landing re-ignition.

To solve optimal control problems, global and local approaches are distinguished. Global methods, such as the HJB approach, do not require any initial guess of the solution and provide a global optimum.[8] However, since these methods are time consuming for problems of high dimension, they cannot be used for real time computations. Local approaches only depend on necessary conditions of optimality. They can be split in two main classes of methods: indirect methods rely on the application of the Pontryagin's Maximum Principle[10] and consist of solving a two-point boundary value problem by finding the zero of a function, direct methods mainly consist of discretizing the state and the control to turn the problem into an optimization problem with constraints.[1] Unlike direct methods, indirect methods are known to be efficient in big dimensions while providing very precise solutions using a Newton algorithm. However, these methods, often based on a shooting algorithm, are known to be very sensitive to the initial guess of the solution. The main contribution of this work is the numerical solution that tackles this initialization problem using homotopy techniques coupled with a multiple shooting algorithm.[6,13]

First, the shooting algorithm is used to compute a reference trajectory that includes: the first re-ignition for the return boost; a ballistic phase; the intermediate boost to satisfy pure state constraints on the dynamic pressure, the thermal flow and the load factor; and the atmospheric re-entry (see Figure 1). The landing burn is not considered in this paper. A mixed constraint (control and state constraint) on the angle of attack is considered as well. This reference trajectory, obtained offline, is used to initialize the guidance algorithm which consists of recomputing the optimal control online using the measured state at each time. The solution obtained at the previous sample time is used

Copyright © 2019 by E. Brendel, B. Hérissé and E. Bourgeois. Published by the EUCASS association with permission.

to initialize the problem at the current time. This procedure ensures fast computations using the fact that solutions are very close to each other providing that the sample time is small enough. The results obtained in simulation are very promising. In particular, they have shown that computing optimal guidance from the reference trajectory provides solutions very quickly, at a frequency that is compatible with actual embedded solutions.

In Section 2, the system dynamics is provided and the optimal control problem is presented. Section 3 presents the numerical method, based on the Pontryagin Maximum Principle, that is used to solve the problem. In Section 4, the optimal control solution is analyzed in details. Section 5 provides some numerical results to demonstrate the effectiveness of the full guidance algorithm.

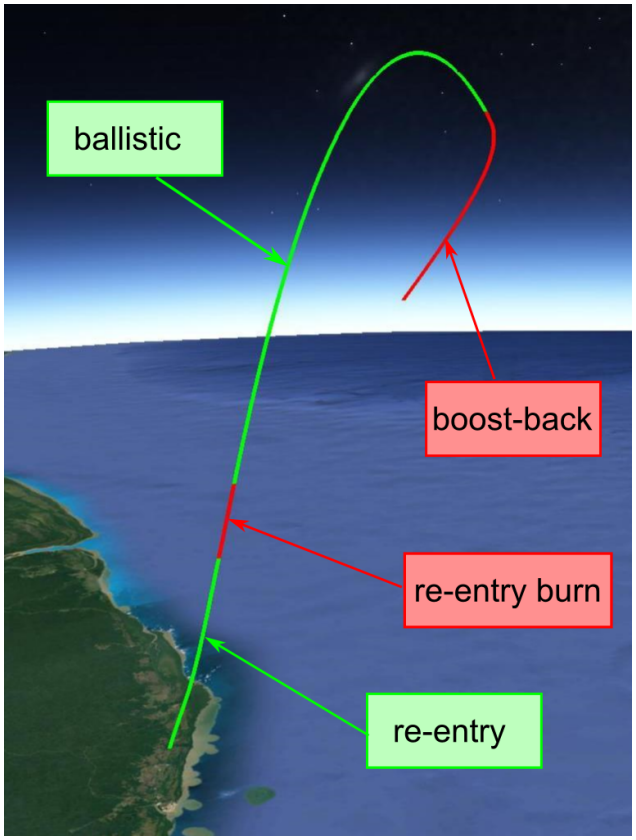

Figure 1: Return trajectory for the Toss Back concept

2. Problem modeling

In this section, the vehicle's dynamics are exposed and the optimal control problem is stated.

2.1 General model

The dynamics of the first stage of the vehicle are given in the Earth-Centered Earth-Fixed (ECEF) coordinates system,

$$\left\{\begin{array}{rcl} \dot{r} & = & v, \\ \dot{v} & = & [a]_{ECEF} - 2\Omega \times v - \Omega \times (\Omega \times r), \\ \dot{m} & = & -q_m \gamma, \end{array}\right. \tag{1}$$

where the acceleration is

$$[a]_{ECEF} = \frac{L(r,v,\alpha,\gamma)}{m}\frac{k}{||k||} - \frac{D(r,v,\alpha,\gamma)}{m}\frac{v}{||v||} - g(r) + \frac{T_m - A_e P_a(r)}{m}\gamma u, \tag{2}$$

and,

$$k = \left(\frac{v}{\|v\|} \times u\right) \times \frac{v}{\|v\|}, \tag{3}$$

$r(t) \in \mathbb{R}^3$ is the position of the vehicle, $v(t) \in \mathbb{R}^3$ is its velocity and $m(t) > 0$ is its mass. $\Omega \in \mathbb{R}^3$ is Earth's rotational velocity. $q_m > 0$ is the maximal mass flow rate of the engine, $T_m > 0$ is the maximal thrust (function of q_m and of the specific impulse), $A_e > 0$ is the nozzle exit area, the orientation of the thrust is represented by the unit vector $u(t) \in \mathbb{R}^3$ and $\gamma(t) \geqslant 0$ is the normalized thrust such that $|\gamma| < 1$. The ambient pressure is noted $P_a(r)$. The gravitational acceleration is modeled by the vector

$$g(r) = \frac{\mu_0}{\|r\|^3} r, \tag{4}$$

where μ_0 is the Earth gravitational constant. Variables $L(r, v, \alpha, \gamma) \geqslant 0$ and $D(r, v, \alpha, \gamma) > 0$ are respectively the lift force and the drag force. $\alpha(t)$ is the angle between the principal axis of the vehicle and the vector $v(t)$.

2.2 Aerodynamic forces

At the re-entry phase, the thrust vector has the same direction as the velocity vector. Then, due to coupled aerodynamic-thrust effects, aerodynamic forces depend on the thrust. Modeling these forces is very difficult in general since it involves complex Computational Fluid Dynamics (CFD) analysis. In this study, for simplicity, a linear dependency was adopted for modeling the effect that the aerodynamic forces decrease when the thrust increase. Thus, a multiplicative factor $(1 - \gamma)$ applied to the aerodynamic forces is used to model the impact of thrust during the atmospheric re-entry. Therefore, when the engine is off ($\gamma = 0$), the aerodynamic forces are fully active, and when the thrust is maximal ($\gamma = 1$), the aerodynamic forces disappear. This model is not fully realistic but allows to compute an optimal trajectory with an intermediate boost consistent with intermediate boosts observed during SpaceX Falcon 9 first stage recovery. This model is irrelevant during the first boost (the boost which provides the velocity vector inversion) but due to an insignificant atmospheric density at these phase and altitude, the aerodynamic forces are negligible in comparison with the other forces, therefore the model is still appropriate. Thus, aerodynamic forces are written

$$\begin{cases} L(r, v, \alpha, \gamma) &= (1 - \gamma) L(r, v, \alpha), \\ D(r, v, \alpha, \gamma) &= (1 - \gamma) D(r, v, \alpha), \end{cases} \tag{5}$$

with

$$\begin{cases} L(r, v, \alpha) &= \frac{1}{2}\rho(r) S_{\text{ref}} C_L(\alpha, M)\|v\|^2, \\ D(r, v, \alpha) &= \frac{1}{2}\rho(r) S_{\text{ref}} C_D(\alpha, M)\|v\|^2, \end{cases} \tag{6}$$

where $\rho(r) > 0$ is the atmospheric density, and $S_{\text{ref}} > 0$ is the reference surface of the vehicle. $C_L(\alpha, M)$ and $C_D(\alpha, M)$ are respectively the lift coefficient and the drag coefficient ; they depend on the angle of attack α and the Mach number $M = \|v\|/v_s(r)$, where $v_s(r)$ is the sound velocity in the air at the position r.

In this paper, the model for $C_L(\alpha, M)$ and $C_D(\alpha, M)$ is written as follows[11]

$$\begin{cases} C_L(\alpha, M) &= C_{L_1}(\alpha, M) \sin(2\alpha), \\ C_D(\alpha, M) &= C_{D_0}(\alpha, M) + 2C_{L_1}(\alpha, M) \sin^2(\alpha), \end{cases} \tag{7}$$

such that

$$C_D(\alpha, M) + \frac{C_L(\alpha, M)}{\tan \alpha} = C_{D_0}(\alpha, M) + 2C_{L_1}(\alpha, M) = C_{N_\alpha}(\alpha, M), \tag{8}$$

where C_{N_α} is the gradient (w.r.t. the angle of attack α) of the lift coefficient in the body frame and C_{D_0} is the drag coefficient for a null angle of attack. They are considered as constants in this paper. Note that the modeling (7) is not restrictive and is consistent with classical modeling, in particular for small values of the angle of attack. This choice is mainly motivated by the guidance design (see Section 4). It can also be noted that

$$k = u - \cos(\alpha)\frac{v}{\|v\|}, \tag{9}$$

then, the acceleration can be written in the ECEF coordinates system as

$$[a]_{ECEF} = (1 - \gamma)\frac{\rho(r)\|v\|^2 S_{\text{ref}} C_{L_1}}{m} \cos(\alpha) u - (1 - \gamma)\frac{\rho(r)\|v\|^2 S_{\text{ref}} C_{N_\alpha}}{2m}\frac{v}{\|v\|} - g(r) + \frac{T_m - A_e P_a(r)}{m}\gamma u. \tag{10}$$

An advantage of this model is that the aerodynamic forces in Equation (10) can be split in two terms with one term that does not depend on the control u.

2.3 Atmospheric density and ambient pressure

The atmospheric density model is

$$\rho(r) = \rho_0 \exp\left(\frac{\|r\| - R_E}{h_r}\right), \tag{11}$$

and the ambient pressure model is

$$P_a(r) = p_0 \exp\left(\frac{\|r\| - R_E}{h_r}\right), \tag{12}$$

where ρ_0 (resp. p_0) is the sea level atmospheric density (resp. the sea level atmospheric pressure), R_E is the Earth's radius and h_r is a reference altitude. This exponential model is used for simplicity, however, there is no technical difficulty preventing from using a more realistic model provided that the functions modeling ρ and P_a are sufficiently smooth to ensure numerical convergence of the algorithm described in Section 3.

2.4 Constraints

The dynamic pressure is introduced

$$Q = \frac{1}{2}\rho(r)\|v\|^2, \tag{13}$$

as well as the thermal flow

$$\Phi = \Phi_0 \sqrt{\rho(r)}\|v\|^{3.15}, \tag{14}$$

and the load factor

$$\eta = \frac{g(r) + \dot{v}}{\|g(r)\|}. \tag{15}$$

From guidance point of view, the dynamics in attitude will be considered as being perfect: the orientation of the thrust will follow instantaneously the motion of the longitudinal axis of the vehicle. Hence, the angle of attack can be defined by the equations

$$\left\{\begin{array}{rcl} \cos(\alpha) & = & u \cdot \frac{v}{\|v\|}, \\ \sin(\alpha) & = & u \cdot \frac{k}{\|k\|}. \end{array}\right. \tag{16}$$

The following constraints on the angle of attack, dynamic pressure, thermal flow and load factor have to be respected during the flight

$$\left\{\begin{array}{rcl} Q & \leqslant & Q_{\max}, \\ \Phi & \leqslant & \Phi_{\max}, \\ \eta_x = |\eta \cdot u| & \leqslant & \eta_{x_{\max}}, \\ \eta_z = \|\eta \times u\| & \leqslant & \eta_{z_{\max}}, \\ \alpha & \in & [\pi - \alpha_{\max}, \pi] \text{ if } \|r\| \leqslant r_{\min}, \end{array}\right. \tag{17}$$

where $Q_{\max}$, $\Phi_{\max}$, $\eta_{x_{\max}}$, $\eta_{z_{\max}}$ and $r_{\min}$ are constants, and $\alpha_{\max}$ is defined to realize a tightening around Mach 1 in order to avoid important disturbances related to the transonic flight:

$$\alpha_{\max} = \alpha_M + (\alpha_m - \alpha_M) \exp\left(-\frac{(M-1)^2}{2\sigma^2}\right), \tag{18}$$

where α_m, α_M and σ are parameters used to define the shape of $\alpha_{\max}$ and M is the Mach number.

2.5 Optimal control problem

The recovery of the first stage of the vehicle starts with a fixed initial state, coinciding with the position $r_0 \in \mathbb{R}^3$, the velocity $v_0 \in \mathbb{R}^3$ and the mass $m_0 \in \mathbb{R}_+$ of the first stage at the end of the ascent phase of flight. The goal of the recovery is to bring the first stage back to a final position $r_f \in \mathbb{R}^3$ just before the landing boost (the landing boost is not considered in this paper) with a penalized velocity close to a reference final velocity $v_f \in \mathbb{R}^3$ while minimizing the first stage's propellant consumption along the return trajectory. The vehicle is supposed not propelled at the end of the trajectory (the landing is not considered here), that is why a fixed final velocity vector would be difficult to obtain. The penalization of the final velocity vector is a good trade-off between a feasible control problem (i.e. an admissible solution exists) and the reach of a desired velocity. Finally, the pure state constraints and the mixed constraints exposed in Equation (17) have to be ensured during the flight.

Hence, the optimal control problem can be summed up as follows:

$$\min \int_0^{t_f} \gamma dt + k_{v_f} \left\| v\left(t_f\right) - v_f \right\|^2 \text{ such that } \begin{cases} (r(\cdot), v(\cdot), m(\cdot)) \text{ is the solution of Equation (1),} \\ (r, v, m)(0) = (r_0, v_0, m_0)\,, \\ r\left(t_f\right) = r_f, \\ t_f, m\left(t_f\right) \text{ and } v\left(t_f\right) \text{ are free,} \\ \text{the constraints of Equation (17) are respected along the trajectory,} \end{cases} \tag{19}$$

where k_{v_f} is a tuning parameter for the velocity penalization.

3. Method statement

Pontryagin's Maximum Principle[10] provides a rewriting of the optimal control problem stated in Equation (19) into an initialization and zero-finding problem. A co-state of the system is introduced and its dynamics are deduced from the study of the Hamiltonian of the system. Then, Pontryagin's Maximum Principle provides necessary optimality conditions in the form of a function of the initial value of the co-state vector. If the initial value of the co-state vector is a zero of this function, the corresponding trajectory verifies the necessary optimality conditions of Pontryagin's Maximum Principle. This zero is sought, for example, with a Newton-Raphson method.

The indirect method provides a high numerical precision and a fast convergence comparing to direct methods. Nevertheless, a prior knowledge of the structure of the solution and a good initialization are needed for the success of this method. Therefore, to tackle this problem in this paper, a simplified problem whose the solution can be computed explicitly is first considered, and the complete optimal control problem (19) is reached by a continuation method[2] by adding the previously neglected terms. The continuation method consists in solving optimal control problems by slightly changing the problem at each iteration while initializing the new problem with the previously computed solution.

3.1 Pontryagin's Maximum Principle with pure state constraints and mixed constraints

The necessary optimality conditions provided by the application of Pontryagin's Maximum Principle to the optimal control problem (Equation (19)) are briefly given in this section.[7,12]

The complete optimal control problem (Equation (19)) can be rewritten as

$$\min \int_0^{t_f} f^0(X, U, t)dt + g\left(X\left(t_f\right), t_f\right) \text{ such that } \begin{cases} \dot{X} = f(X, U, t), \\ X(0) = X_0,\ r\left(t_f\right) = r_f, \\ t_f, m\left(t_f\right) \text{ and } v\left(t_f\right) \text{ are free,} \\ \forall t,\ c_p(X(t)) \leqslant 0, \\ \forall t,\ c_m(X(t), U(t)) \leqslant 0, \end{cases} \tag{20}$$

where $X = (r, v, m)$, $U = (u, \gamma)$, f^0 (resp. g) is the integral cost function (resp. the final cost function), c_p (resp. c_m) is the pure state constraint function (resp. the mixed constraint function) deduced from Equation (17). In this paper, only the pure state constraint on the dynamic pressure Q and the mixed constraint on the angle of attack α are considered in the optimal control problem for simplicity. The other constraints on the load factor and the thermal flow can be addressed in a similar way.

The co-state vector is denoted $p = (p_r, p_v, p_m) \in \mathbb{R}^3 \times \mathbb{R}^3 \times \mathbb{R}$. The Hamiltonian of the problem (20) is

$$H = p \cdot f(X, U, t) + p^0 f^0(X, U, t). \tag{21}$$

The extended Hamiltonian including the constraints is

$$\tilde{H} = H + \mu_p c_p(X) + \mu_m c_m(X, U). \tag{22}$$

The dynamics of the co-state vector are

$$\dot{p} = -\frac{\partial \tilde{H}}{\partial X}. \tag{23}$$

The minimization condition given by Pontryagin's Maximum Principle is

$$H\left(t, X, p, p^0, U\right) = \min_{V \in \Omega} H\left(t, X, p, p^0, V\right). \tag{24}$$

Furthermore, according to Pontryagin's Maximum Principle, if f and f^0 do not explicitly depend on the time t, then the Hamiltonian H is constant. Also, if the final time t_f is free, then $H(t_f) = 0$. Finally, because $v\left(t_f\right)$ and $m\left(t_f\right)$ are free, the following transversality conditions can be deduced

$$\begin{array}{rcl} p_v\left(t_f\right) & = & p^0 \frac{\partial g}{\partial v}\left(t_f, X\left(t_f\right)\right), \\ p_m\left(t_f\right) & = & p^0 \frac{\partial g}{\partial m}\left(t_f, X\left(t_f\right)\right). \end{array} \tag{25}$$

The mixed constraint function c_m is assumed to be regular, i.e. it verifies the Mangasarian-Fromovitz constraint qualification.[5] In the extended Hamiltonian (Equation (22)), μ_p and μ_m are continuous mapping such that $\mu_p c_p = 0$ and $\mu_m c_m = 0$ for all t. At every contact point t_i with the boundary of the pure state constraint (i.e. when $c_p = 0$), $\tilde{H}$ is continuous and there exists ν_i such that

$$p\left(t_i^+\right) = p\left(t_i^-\right) - \nu_i \frac{\partial c_p}{\partial X}\left(X\left(t_i\right)\right). \tag{26}$$

3.2 Continuation method

Numerically, the multiple necessary conditions of optimality are written as a zero-finding problem where the function for which the zero is sought depends on the initial value of the co-state vector p. Hence, a Newton-Raphson algorithm is used to solve this optimal control problem. However, in order to converge, this algorithm needs a good initialization of the co-state vector p as an input. That is why a continuation method is applied. First, a simplified problem for which an explicit solution can be obtained is used to initialize the co-state vector.[6] Then, every neglected term is gradually added until the problem being solved corresponds to the complete initial problem (19). At each step, a new solution is computed by the Newton-Raphson algorithm and this solution is used as an initialization for the next step.

3.3 Multiple shooting method

A shooting algorithm is generally used to solve optimal control problems by indirect methods.[13] It consists of integrating the extended dynamics (state dynamics (1) and co-state dynamics (23)) of the problem to evaluate the function of the two point boundary problem whose the zero is searched. However, when discontinuities appear in the co-state function and the control, simple shooting is not possible. Such problems typically occur when the optimal control problem includes pure state constraints; or when there are switching times that typically appear when a L^1 norm is used in the cost (Bang-Bang controls and singular controls appear); or if the system is hybrid.[9] Therefore, additional components have to be included in the function in that case. For example, at the time t_Q where the maximum dynamic pressure is achieved, the constraint $Q(t_Q) - Q_{\max} = 0$ must be added at the contact point. Moreover, it can be interesting to use the multiple shooting technique to improve numerical robustness by reducing the initialization sensitivity.[13]

In practice, multiple shooting consists of cutting the trajectory in several pieces and adding junction conditions. The trajectory $X(t), t \in [0, t_f]$ is cut in N pieces $X_k(t), t \in [t_{k-1}, t_k]$, $k = 1, \ldots, N$, with $t_0 = 0$ and $t_N = t_f$. For $k = N$, transversality conditions (25) and boundary conditions (20) apply. For $k = 1, \ldots, N-1$, the state should be continuous: $X_k(t_k) = X_{k+1}(t_k)$. However, the following conditions have to be ensured on the Hamiltonian and the costate:

- If there is no contact with any constraint at t_k, then the co-state is continuous: $p_k(t_k) = p_{k+1}(t_k)$.

- If there is a contact with a constraint at t_k (see Eq. (26)), then $p_k(t_k) = p_{k+1}(t_k) + \nu_k \frac{\partial c_p}{\partial X}(X(t_k))$. Since ν_k is impossible to compute in practice, we rather write the following conditions:

$$\begin{aligned} \Pi_{\frac{\partial c_p}{\partial X}(X(t_k))}(p_k(t_k) - p_{k+1}(t_k)) = 0, \\ c_p(X(t_k)) = 0, \end{aligned} \tag{27}$$

  where $\Pi_u(\cdot)$ is the projection onto the plane orthogonal to the vector u.

- If the time t_k is free, then $H_k(t_k) = H_{k+1}(t_k)$.

4. Solution of the optimal control problem

4.1 Structure of the solution

After studying the structure of the solution, the optimal control along the optimal trajectory of the complete problem is identified. The trajectory is divided into 5 phases (1: first boost, 2: first ballistic phase, 3: intermediate boost, 4a: ballistic phase before reaching the contact point $Q = Q_{\max}$, 4b: ballistic phase after reaching this contact point) with switching times between them. The following subsections describe the optimal control for each phase.

4.1.1 Computation of the control input with negligible aerodynamic forces (phases 1 and 2)

First, in order to compute the optimal control, the aerodynamic forces are assumed to be negligible during these phases. This hypothesis is relevant because the vehicle has a high altitude during these phases. Hence, in the Hamiltonian, the expression depending on the control input (γ, u) is

$$J_1 = \gamma\left(1 - q_m p_m + \frac{T_m - A_e P_a(r)}{m}(p_v \cdot u)\right), \tag{28}$$

and according to Pontryagin's Maximum Principle, the optimal control input (γ, u) minimizes J_1. Therefore,

$$u = -\frac{p_v}{\|p_v\|}$$

and

$$J_1 = \gamma\left(1 - q_m p_m - \frac{T_m - A_e P_a(r)}{m}\|p_v\|\right). \tag{29}$$

The switching function Ψ is defined as

$$\Psi = 1 - q_m p_m - \frac{T_m - A_e P_a(r)}{m}\|p_v\|. \tag{30}$$

Then, because the input γ minimizes $J_1 = \gamma\Psi$, the value of γ can be deduced from the sign of Ψ, i.e. if $\Psi < 0$ then $\gamma = 1$, and if $\Psi > 0$ then $\gamma = 0$. The case where $\Psi = 0$ is irrelevant in this paper, there is no singular trajectory and then Ψ is never equal to zero on a nonempty interval.

The optimal control for the first two phases of the flight can be deduced from this study: a first boost providing the velocity vector inversion ($\gamma = 1$ and $u = -p_v/\|p_v\|$) followed by a ballistic phase ($\gamma = 0$ and $u = -p_v/\|p_v\|$).

4.1.2 Computation of the control input for the intermediate boost (phase 3)

The hypothesis on the negligible aerodynamic forces is not relevant anymore for this phase even if they remain low compared to the thrust force. However, the coupling between u and γ in the expression of the lift force complicates the explicit computation of the optimal control input. Then, the optimal control needs to be approximated: the expression of the input $u = -p_v/\|p_v\|$ is the same as in the first two phases, it is justified using the fact that aerodynamic forces remain low and the switching function is now

$$\Psi = 1 - q_m p_m - \frac{T_m - A_e P_a(r)}{m}\|p_v\| + \frac{\rho(r)\|v\|S_{\text{ref}}}{2m} C_{D_0}(v \cdot p_v). \tag{31}$$

The analysis of the switching function Ψ shows that the trajectory can be singular during this phase, but the explicit computation of the corresponding input γ is mathematically complex. That is why a constant approximation is taken

for the value of γ along this phase. It has been checked that the gain in terms of cost (of the optimal control problem) would have been negligible with the exact expression of the singular control input.

This intermediate boost is such that the boundary of the dynamic pressure constraint is reached at a single contact point. In other words, there does not exist a nonempty interval I in $\left[0, t_f\right]$ such that $Q(t) = Q_{\max}$ in I. Then, the Lagrange multiplier μ_p has not to be dealt with, because for all time t, $\mu_p(t)\,(Q(t) - Q_{\max}) = 0$.

4.1.3 Computation of the control input during atmospheric re-entry (phase 4)

The atmospheric re-entry is a ballistic phase, i.e. $\gamma = 0$. The lift force is considered, then the expression depending on the control input (γ, u) in the Hamiltonian is

$$J_4 = \frac{\rho(r)\|v\|S_{\text{ref}}C_{L_1}}{m}\,(u \cdot v)\,(u \cdot p_v)\,. \tag{32}$$

Therefore, the control input u which minimizes J_4 can be explicitly computed to minimize the Hamiltonian.

In an algorithmic point of view, this phase is composed of two phases 4a and 4b. The expression of the control input is the same in both phases but the switching time t_4 between these two phases is needed to deal with the contact point of the dynamic pressure Q at the boundary of the constraint $Q = Q_{\max}$. The conditions related to t_4 are presented in Section 4.1.5.

4.1.4 Saturation of the angle of attack

As soon as the altitude of the vehicle is inferior to an altitude $r_{\min}$, the constraint on the angle of attack (see Equation (17)) is applied. Hence, if $\|r\| \leqslant r_{\min}$ and if $\alpha < \pi - \alpha_{\max}$, the orientation of the thrust u is saturated in order to have $\alpha = \pi - \alpha_{\max}$, then the expression of u is

$$u = \cos\left(\pi - \alpha_{\max}\right) e_v + \sin\left(\pi - \alpha_{\max}\right) e_v^{\perp}, \tag{33}$$

where $e_v = v/\|v\|$ and $e_v^{\perp} = (v \times (p_v \times v)) \,/\, \|v \times (p_v \times v)\|$.

When this mixed constraint is active,

$$c_m(v, u) = \cos(\alpha) + \cos(\alpha_{\max}) = u \cdot \frac{v}{\|v\|} + \cos(\alpha_{\max}) = 0.$$

Then, a term needs to be added to the expression of the dynamics of the velocity co-state p_v as presented in Section 3.1:

$$\dot{p}_v = -\frac{\partial \tilde{H}}{\partial v} = -\frac{\partial H}{\partial v} - \mu_m \frac{\partial c_m}{\partial v}(v, u). \tag{34}$$

The Lagrange multiplier μ_m is computed by noticing that for this application, $\tilde{H} = 0$ for all t, and then μ_m can be deduced from $d\tilde{H}/dt = 0$ for all t.

4.1.5 Optimality necessary conditions on the switching times and the final time using Pontryagin's Maximum Principle

As presented in Sections 4.1.1, 4.1.2 and 4.1.3, the trajectory is divided into 5 phases (first boost, first ballistic phase, intermediate boost, ballistic phase before reaching the contact point $Q = Q_{\max}$, ballistic phase after reaching this contact point) with switching times between them. The necessary conditions of optimality provided by Pontryagin's Maximum Principle give conditions on the optimal switching times (see Section 3.3), on the final time, and allow their computation by the Newton-Raphson algorithm.

4.2 Co-state initialization for a simplified problem

As presented in Section 3.2, a simplified optimal control problem is explicitly solved in order to initialize the multiple continuation steps. This simplified optimal control problem is

$$\min \int_0^{t_f} \gamma^2 dt \text{ such that } \begin{cases} \begin{cases} \dot{r} &= v, \\ \dot{v} &= \frac{T_m}{m}\gamma u, \end{cases} \\ (r, v)(0) = (r_0, v_0)\,, \\ r\left(t_f\right) = r_f,\ t_f \text{ is fixed}, \\ v\left(t_f\right) \text{ is free}. \end{cases} \tag{35}$$

It is straightforward to show that the solution of problem (35) is

$$\begin{cases} u &= -\frac{p_v}{\|p_v\|}, \\ \gamma &= \frac{T_m}{2m}\|p_v\|, \end{cases} \tag{36}$$

with the initial co-states

$$\begin{cases} p_r(0) = p_r = -\frac{6m^2}{T_m^2 t_f^3}\left(r_f - r_0 - t_f v_0\right), \\ p_v(0) = t_f p_r. \end{cases} \tag{37}$$

Starting from this simplified problem, every missing parameter is added by continuation method (see Section 3.2) until the problem being solved is the problem presented in Equation (19). Thus, parameters modeling the gravity acceleration, the aerodynamic forces, the cost function and the constraints are added sequentially to obtain the expected solution.

5. Results

5.1 Reference trajectory computed offline

The results presented in this section are computed using the method exposed in Section 3. The results are presented with normalized values. The order of magnitude for the initial altitude is 8×10^4 m, 2×10^3 m.s^{-1} for the initial velocity norm, 10^5 m for the initial range, and 4×10^4 kg for the final consumed mass, The optimal altitude of the vehicle in function of its range to the landing platform is presented in Figure 2 with each color corresponding to a guidance phase.

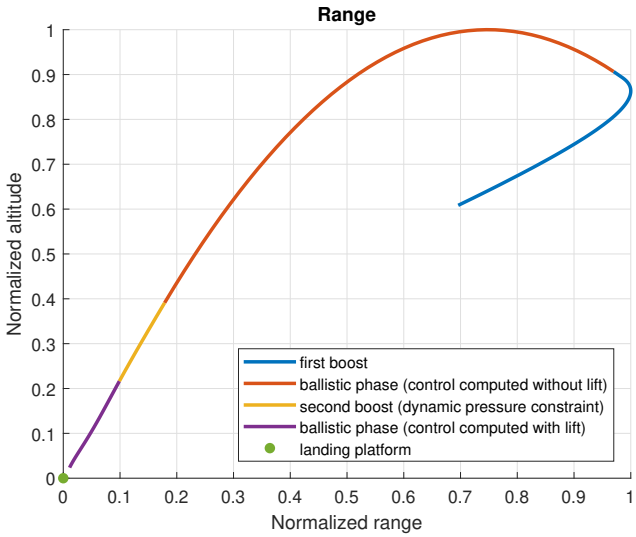

Figure 2: Altitude of the vehicle in function of its range to the landing platform

The corresponding optimal control input (u, γ) is presented in Figure 3, where the different phases are separated by the switching times $t_{1,\dots,4}$ with t_4 the time where the maximal atmospheric pressure is achieved. The orientation of the thrust vector u is presented in the ECEF coordinates system. Two discontinuities can be observed, the first around 70% of the final time is a consequence of the saturation of the angle of attack, and a second one at the switching time t_3, because the lift force is taken into account from t_3 and changes the expression of the optimal control input u (see Section 4.1.3).
It should be recalled that only the pure state constraint on the dynamic pressure (Figure 4(a)) and the mixed constraint on the angle of attack (Figure 4(e)) have been considered. That is why the constraint on the longitudinal loading factor is not verified (Figure 4(c)) for all time. However, the constraints on the thermal flow (Figure 4(b)) and the lateral load factor (Figure 4(d)) are respected.

5.2 Simulation results of the guidance algorithm with scattered parameters

In this section, a vehicle with randomly scattered parameters (for example, initial state dispersion, aerodynamic coefficients, maximal thrust, maximal mass flow rate...) is simulated in a more realistic environment.

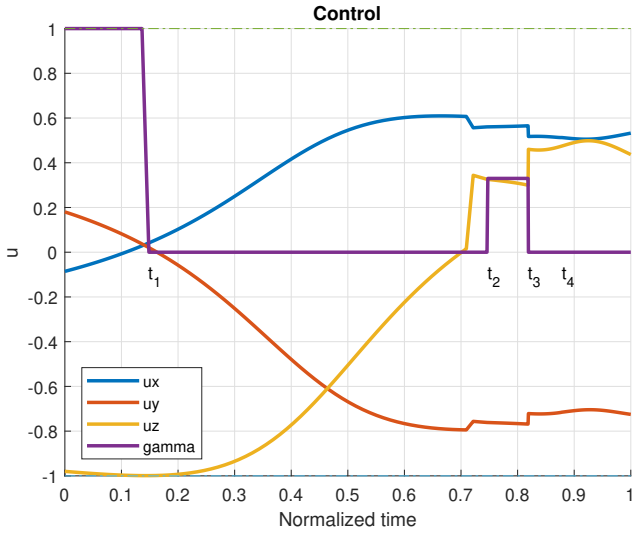

Figure 3: Optimal control input (u, γ)

The guidance algorithm consists of re-computing an optimal control at each sample time to obtain a closed-loop algorithm. Briefly, the optimal control input is periodically re-computed using the method detailed in Section 3. A continuation method on the vehicle state is performed using the last computed solution, obtained at the previous time, as a guess to update the solution at the current time.

1000 cases have been considered with 100% success rate. The results are presented in Figure 5, where the nominal simulation is presented in red and the Monte-Carlo simulations are presented in blue. The thrust input (see Figure 5(c)) has been set to 95% of its real maximal value in order to keep the ability to maneuver in case of perturbations. The results show that, despite uncertainties on the system parameters, the precision of the guidance algorithm is satisfactory since the final position is about 100 m around the desired position and the velocity is about 10 m.s^{-1} around the desired one. This level of performance is possible because the low-lift maneuver capability of the vehicle has been exploited during the re-entry. Moreover, the observed computation times show that a real-time implementation of the optimal guidance algorithm is possible at a frequency around 1 Hz.

6. Conclusion

An optimal guidance algorithm with an indirect shooting method based on Pontryagin's Maximum Principle has been applied to the re-entry of a Toss Back Reusable Launch Vehicle, from the beginning of the first boost to the time before the landing boost. This algorithm provides a computation of the control input and the trajectory which minimize the consumed mass. A reference trajectory was computed offline, then this algorithm was adapted to provide a closed-loop guidance algorithm that has been simulated in a more realistic physical environment. Model and mission parameters were scattered in order to demonstrate the effectiveness and the robustness of the presented method, which converged in 100% of the cases. Nevertheless, it would be worth improving the representativeness of the model considered for simulation in order to assess the impact on the guidance performance.

A direct improvement of the algorithm would consist of including the unconsidered constraints on the load factor and the thermal flow. To go further, a more realistic model of the system should be considered. For example, a better model of the rocket engine could be used considering transient effects. Also, a finer model of the aerodynamic forces should be considered, taking into account the dependency on the Mach number in particular. A better modeling of the atmospheric pressure would also improve the performance of the guidance algorithm. Although those improvements will increase the overall performance and the representativeness of the solution, the complexity of the algorithm will also increase, then a trade-off will have to be determined to keep real time capabilities.

Another future prospect would be to adapt the algorithm to the low computation means available on the hardware of that type of vehicle. Finally, the method could be tested in hardware-in-the-loop simulations and embedded in a future launch of a demonstrator.

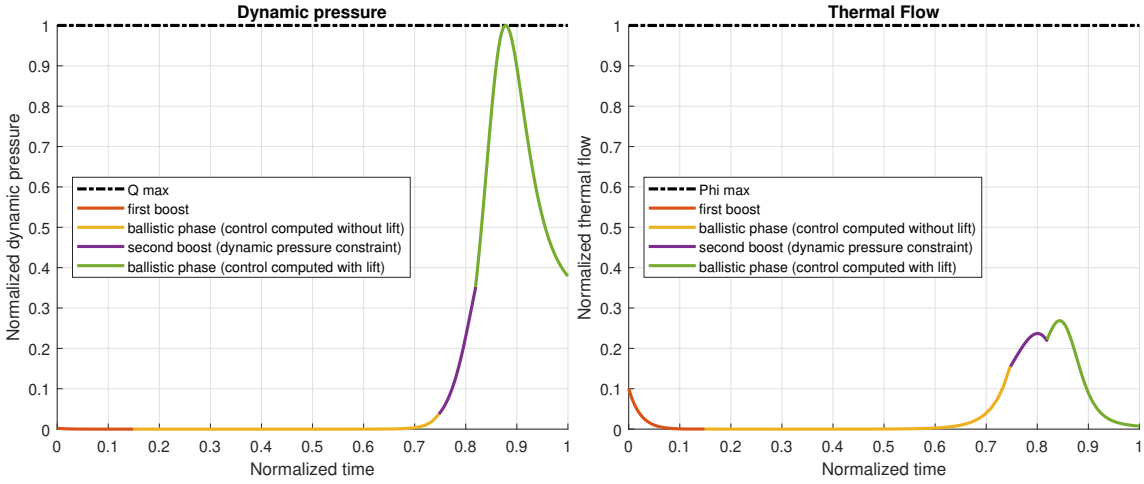

(a) Dynamic pressure

(b) Thermal flow

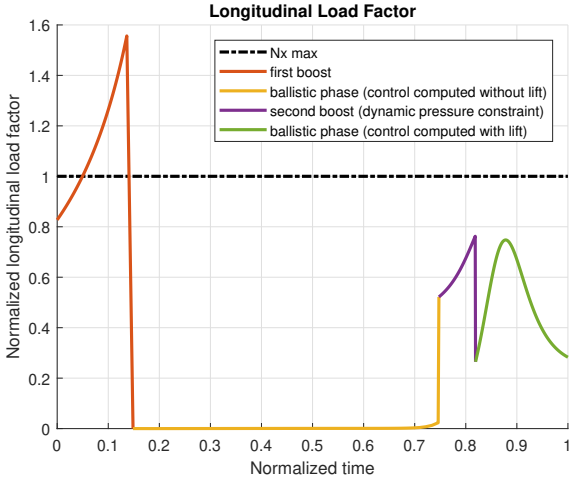

(c) Longitudinal load factor

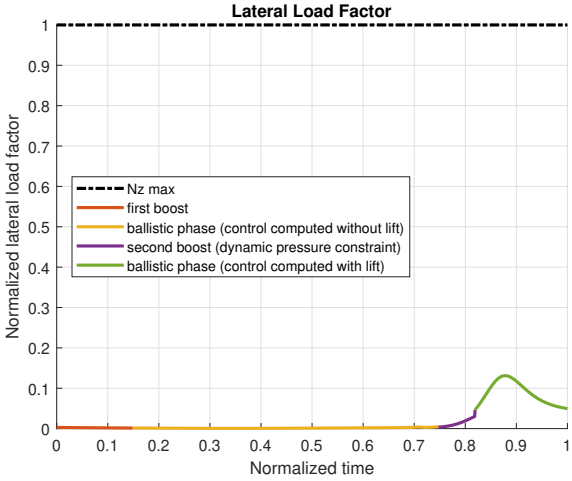

(d) Lateral load factor

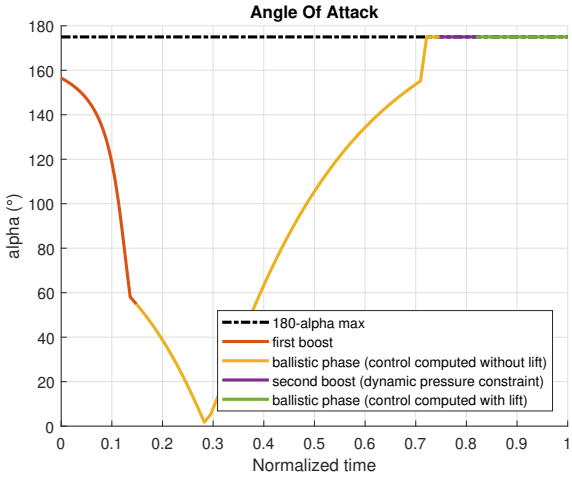

(e) Angle of attack

Figure 4: Constraints from Equation (17)

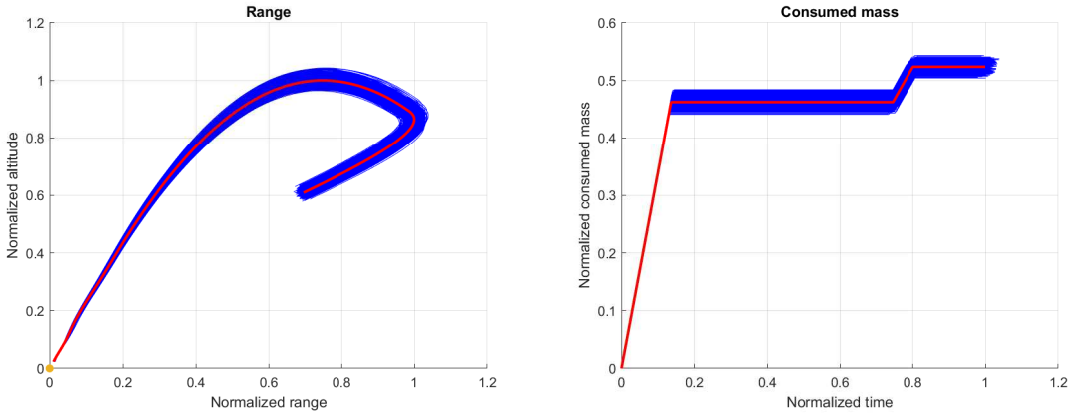

(a) Altitude in function of the range

(b) Consumed mass

(c) Control input γ

(d) Velocity norm

Figure 5: Monte-Carlo simulations

References

[1] B. Acikmese and S. R. Ploen. Convex programming approach to powered descent guidance for mars landing. *Journal of Guidance, Control, and Dynamics*, 30(5):1353–1366, 2007.

[2] E. L. Allgower and K. Georg. *Numerical Continuation Methods - An Introduction*. Springer-Verlag Berlin Heidelberg, 2003. ISBN 978-3-642-61257-2.

[3] P. Baiocco and Ch. Bonnal. Technology demonstration for reusable launchers. *Acta Astronautica*, 120:43–58, 12 2015.

[4] L. Blackmore. Autonomous precision landing of space rockets. *The Bridge*, 4(46):15–20, 01 2016.

[5] R. Bonalli. *Optimal control of aerospace systems with control-state constraints and delays*. PhD thesis, Sorbonne Université, UPMC University of Paris 6; ONERA–The French Aerospace Lab, 2018.

[6] R. Bonalli, B. Hérissé, and E. Trélat. Analytical initialization of a continuation-based indirect method for optimal control of endo-atmospheric launch vehicle systems. In *IFAC World Congress*, volume 50, pages 482–487. Elsevier, 2017.

[7] B. Bonnard, L. Faubourg, G. Launay, and E. Trélat. Optimal control with state constraints and the space shuttle re-entry problem. *Journal of Dynamical and Control Systems*, 9 (2):155–199, 2003.

[8] E. Bourgeois, O. Bokanowski, H. Zidani, and A. Désilles. New improvements in the optimization of the launcher ascent trajectory through the hjb approach. In *EUCASS*, 2017.

[9] T. Haberkorn and E. Trélat. Convergence results for smooth regularizations of hybrid nonlinear optimal control problems. *SIAM Journal on Control and Optimization*, 49(4):1498–1522, 2011.

[10] L. S. Pontryagin. *Mathematical theory of optimal processes*. CRC Press, 1987.

[11] D. Pucci, T. Hamel, P. Morin, and C. Samson. Nonlinear feedback control of axisymmetric aerial vehicles. *Automatica*, 53:72 – 78, 2015.

[12] E. Trélat. *Contrôle optimal : théorie & applications*. Vuibert, 2005. ISBN 2 7117 7175 X.

[13] E. Trélat. Optimal control and applications to aerospace: Some results and challenges. *JOTA*, 154(3), 2012.